Structure and Function of Transmembrane Segment XII in Osmosensor and Osmoprotectant Transporter ProP of *Escherichia coli*†

Feng Liu,‡,§ Doreen E. Culham,|| Yaroslava I. Vernikovska,‡ Robert A. B. Keates,|| Joan M. Boggs,‡ and Janet M. Wood*,||

Department of Structural Biology and Biochemistry, Hospital for Sick Children, Toronto M5G 1X8, ON Canada, Department of Laboratory Medicine and Pathobiology, University of Toronto, Toronto M5G 1L5, ON Canada, and Department of Molecular and Cellular Biology and Guelph-Waterloo Centre for Graduate Work in Chemistry and Biochemistry, University of Guelph, Guelph N1G 2W1, ON Canada

Received October 23, 2006; Revised Manuscript Received March 13, 2007

ABSTRACT: *Escherichia coli* transporter ProP acts as both an osmosensor and an osmoregulator. As medium osmolality rises, ProP is activated and mediates H^+-coupled uptake of osmolytes like proline. A homology model of ProP with 12-transmembrane (TM) helices and cytoplasmic termini was created, and the protein's topology was substantiated experimentally. Residues 468−497, at the end of the C-terminal domain and linked to TM XII, form an intermolecular, homodimeric α-helical coiled-coil that tunes the transporter's response to osmolality. We aim to further define the structure and function of ProP residues Q415−E440, predicted to include TM XII. Each residue was replaced with cysteine (Cys) in a histidine-tagged, Cys-less ProP variant (ProP*). Cys at positions 415−418 and 438−440 were most reactive with Oregon Green Maleimide (OGM), suggesting that residues 419 through 437 are in the membrane. Except for V429−I433, reactivity of those Cys varied with helical periodicity. Cys predicted to face the interior of ProP were more reactive than Cys predicted to face the lipid. The former may be exposed to hydrated polar residues in the protein interior, particularly on the periplasmic side. Intermolecular cross-links formed when ProP* variants with Cys at positions 419, 420, 422, and 439 were treated with DTME. Thus TM XII can participate, along its entire length, in the dimer interface of ProP. Cys substitution E440C rendered ProP* inactive. All other variants retained more than 30% of the proline uptake activity of ProP* at high osmolality. Most variants with Cys substitutions in the periplasmic half of TM XII activated at lower osmolalities than ProP*. Variants with Cys substitutions on one face of the cytoplasmic half of TM XII required a higher osmolality to activate. They included elements of a GXXXG motif that are predicted to form the interface of TM XII with TM VII. These studies define the position of ProP TM XII within the membrane, further support the predicted structure of ProP, reveal the dimerization interface, and show that the structure of TM XII influences the osmolality at which ProP activates.

Cells respond to changes in extracellular osmolality by modulating their cytoplasmic composition. Osmoregulatory transporters and biosynthetic enzymes mediate solute accumulation as osmolality increases. Mechanosensitive channels mediate solute release as osmolality decreases. Archaea (*1*, *2*), eubacteria (*3*, *4*), and eukaryotic cells (*5*−*10*) share these responses.

Osmoprotectants are organic solutes that stimulate microbial growth in high osmolality media. They act as or are converted to compatible solutes, compounds that can accumulate to high cytoplasmic levels without impairing cellular function. Three osmoprotectant transporters have been expressed, purified, and reconstituted into proteoliposomes: major facilitator superfamily (MFS[1]) member ProP of *Escherichia coli* (*11*), betaine-carnitine-choline transporter (BCCT) family member BetP of *Corynebacterium glutamicum* (*12*), and ATP binding cassette (ABC) transporter OpuA of *Lactococcus lactis* (*13*). Each can sense and respond to extracellular osmolality in the absence of other proteins, and each represents a ubiquitous class of molecules that forestall the dehydration of animal, plant, and microbial cells by mediating the uptake of organic solutes.

† This work was supported by Research Grants MOP-42463, IG1-67335, and MOP-68904 awarded to J.M.W. and J.M.B. by the Canadian Institutes of Health Research and a postdoctoral fellowship awarded to F.L. by the Hospital for Sick Children−Research Training Centre.

* Correspondence. Department of Molecular and Cellular Biology, University of Guelph, Guelph, ON N1G 2W1, Canada. Tel: 519 824 4120 ext 53866. Fax: 519 837 1802. E-mail: jwood@uoguelph.ca.

‡ Hospital for Sick Children and University of Toronto.

§ Present address: Department of Biochemistry and Biomedical Sciences, McMaster University, Hamilton, ON, L8N 3Z5, Canada.

|| University of Guelph.

[1] Abbreviations: ΔΨ, membrane potential; ABC transporter, ATP binding cassette transporter; BCCT family, betaine-carnitine-choline transporter family; DNase I, deoxyribonuclease I; CBS, cystathionine-β-synthase; DTME, dithio-bis-maleimidoethane; EDTA, ethylenediamine tetraacetic acid; IPTG, isopropyl-β-D-thiogalactopyranoside; LB, Luria−Bertani medium; MFS, major facilitator superfamily; MOPS, 4-morpholinopropanesulfonic acid; OGM, Oregon Green 488 Maleimide carboxylic acid; PAGE, polyacrylamide gel electrophoresis; PCR, polymerase chain reaction; SDS, sodium dodecyl sulfate; TC, transporter classification; TM, transmembrane segment (a sequence of amino acids that extends from one membrane surface to the other in an integral membrane protein).

10.1021/bi062198r CCC: $37.00
Published on Web 04/19/2007

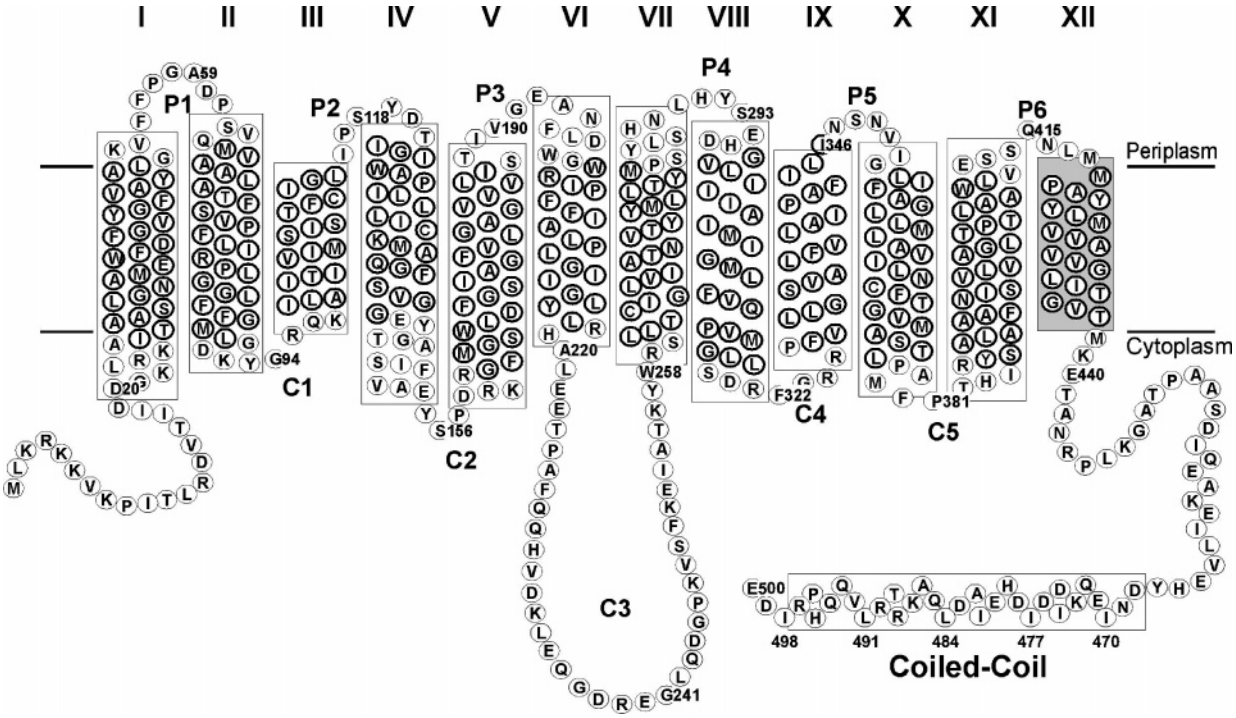

FIGURE 1: The topology of ProP. The illustrated topology is based on a homology model of ProP and substantiated by experimental evidence (*23*). The protein is predicted to form twelve transmembrane (TM) α-helices linked by eleven hydrophilic loops (periplasmic loops P1−P6 and cytoplasmic loops C1−C5). TM XII, the subject of this report, is highlighted by a gray box. Two classes of ProP orthologues are observed (*19*). The C-termini of orthologues typified by *E. coli* ProP terminate in a domain with up to eight of the heptad repeats characteristic of α-helical coiled-coil-forming proteins (*31*). NMR and EPR spectroscopy showed that the synthetic peptide corresponding to *E. coli* ProP residues 468−497 does form a homodimeric, antiparallel α-helical coiled-coil (*28*, *29*), and cross-linking studies were consistent with the occurrence of that structure within ProP dimers, *in vivo* (*30*). The C-terminal domains of orthologues typified by *Corynebacterium glutamicum* ProP (*59*) are shorter and lack the coiled-coil domain.

ProP (TC number 2.A.1.6.4) is a 500 residue integral membrane protein (*14*) and a H^+-osmoprotectant symporter powered by both ΔpH and ΔΨ (*15*−*17*). Its many substrates, all highly water-soluble zwitterions with no net charge, include proline, glycine betaine, and ectoine (*16*). The initial rate of proline uptake via ProP is a sigmoid function of osmolality (not osmotic shift) in both cells and proteoliposomes (*18*). ProP is an osmosensor because chemically diverse, membrane impermeant osmolytes contribute to its activation as they contribute to the osmolality of the external medium (*18*). The same is true of BetP and OpuA (*19*). In proteoliposomes, all three systems respond in an osmolyte-specific manner to the lumenal solvent (*18*, *20*−*22*). Thus the semipermeable membrane transduces the extracellular, osmotic signal to yield a cytoplasmic signal which may be osmosensor-specific (*18*, *19*, *22*). Ultimately such effects must alter the catalytic mechanisms of these transporters, accelerating osmoprotectant transport into cells that face increasing or high osmolality. To fully understand osmosensing, we must correlate the structural dynamics of these proteins with osmoregulation of their transport activities.

Recently we created a homology model for ProP using the crystal structure of *E. coli* GlpT as template (*23*). The predicted topology and orientation of ProP were substantiated by LacZ/PhoA fusion analysis and fluorescent labeling of Cys residues introduced to the termini or the hydrophilic loops linking putative transmembrane helices (*23*). GlpT (*24*) shares a common structural topology with other MFS members including organic anion antiporter OxlT (*25*) and H^+-lactose symporter LacY (*26*). In each structure, TMs III, VI, IX, and XII face the surrounding membrane.

The cytoplasmic C-terminus of ProP is longer than those of its closest paralogues that are not osmosensors or osmoregulators (KgtP and ShiA) (*14*). Extensive structure−function analyses have implicated an α-helical coiled-coil domain at the end of the C-terminus of *E. coli* ProP in the osmoregulation of ProP activity (*14*, *27*−*29*). A peptide corresponding to the ProP C-terminus forms an antiparallel, homodimeric α-helical coiled-coil (*28*) (Figure 1). Cross-linking studies suggest that it is also present in dimers formed by full length ProP, *in vivo* (*30*). Structural modifications that impair coiled-coil formation also elevate the osmolality threshold for ProP activation (*27*, *31*). Recent genomic sequencing has revealed groups of ProP orthologues that do and do not include the coiled-coil structure, though all have extended C-termini. Representatives of both groups share similar osmosensory and osmoregulatory functions (*19*, *31*). Thus the C-terminal coiled-coil is not essential for osmosensing or osmotic activation but it modulates the sensitivity of ProP to medium osmolality. Deletion and mutational analyses have implicated an extended, cytoplasmic C-terminal domain of unknown structure in osmosensing by BetP (*21*, *32*, *33*) and dual cytoplasmic CBS domains in osmosensing by OpuA (*34*).

Formation of a coiled-coil by paired cytoplasmic tails of *E. coli* ProP may affect the structure or environment of residues in TM XII, and some TM XII residues may be located at the dimer interface. In addition, our homology model predicts that five GXXXG motifs occur at interfaces between TMs within each ProP molecule. GXXXG motifs are frequently associated with sites of close helix−helix contact (*35*). A GXXXG motif flanked by G431 and G435

is predicted to occur at the membrane-embedded interface of TM XII with TM VII.

In this study we began to test these predictions by examining ProP residues Q415−E440. A cysteine (Cys) residue was introduced at each site in cysteine-less variant ProP* (*36*) for labeling by Oregon Green Maleimide (OGM), a compound that can react with Cys residues that reside in hydrophilic (but not hydrophobic) environments. The impacts of the Cys replacements on ProP function were also assessed. The OGM reactivities of the introduced Cys were as predicted by our model and revealed the presence of hydrated residues within the membrane core. Several reactive Cys could be cross-linked with dithio-bis-maleimidoethane (DTME) indicating that TM XII participates in the dimer interface. In addition, the Cys substitutions affected the sensitivity of ProP* to medium osmolality.

EXPERIMENTAL PROCEDURES

Materials and Culture Media. Bovine pancreatic DNase I (type II) was from Boehringer-Mannheim (Laval, QC, Canada). Egg white lysozyme (UltraPure grade) was obtained from Caledon Laboratories (Georgetown, ON, Canada). Oligonucleotides were purchased from Cortec DNA Services (Kingston, ON, Canada), and OGM was purchased from Molecular Probes Inc. (Eugene, OR). DTME (dithio-bis-maleimidoethane) was obtained from Pierce Biotechnology Inc. (Rockford, IL). MTSEA (2-aminoethyl-methanethiosulfonate) was from Toronto Research Chemicals (Toronto, ON, Canada). OGM, DTME, and MTSEA were dissolved in *N*,*N*-dimethylformamide (DMF, Fisher Scientific, Nepean, ON, Canada) prior to use and stored at −20 °C, protected from light. Ampicillin, β-mercaptoethanol, and imidazole were from Sigma Chemical Co. (St. Louis, MO). Other reagents were of the highest grade available. Buffers were prepared as described by Racher et al. (*17*), and solution osmolalities were measured with a Wescor vapor pressure osmometer (Wescor, Logan, UT).

Bacteria were cultivated at 37 °C in LB (*37*) or in NaCl-free MOPS medium, a variant of the MOPS medium described by Neidhardt et al. (*38*) from which all NaCl had been omitted. This base medium was supplemented with NH_4Cl (9.5 mM) as nitrogen source and glycerol (0.4% (v/v)) as carbon source. L-Tryptophan (245 μM) and thiamine hydrocholoride (1 μg/mL) were added to meet auxotrophic requirements, creating a complete growth medium with an osmolality of 0.14−0.15 mol/kg. Ampicillin (100 μg/mL) was added as required to maintain plasmids.

Bacteria, Plasmids, and Molecular Biological Manipulations. Basic molecular biological techniques were as described by Sambrook et al. (*39*). Both *proP* expression and ProP activity are osmoregulated (*40*). To focus on the osmoregulation of transporter activity *in vivo*, genes encoding ProP variants were expressed at a physiological level and in an osmolality-independent manner from the AraC-controlled P_{BAD} promoter (*27*). With the same system, arabinose induction allowed us to overexpress and purify variants for site-directed fluorescence labeling experiments (see below) (*17*).

ProP variants were expressed in plasmid-bearing derivatives of *E. coli* WG350 (F^- *trp lacZ rpsL thi* Δ(*putPA*)*101* Δ(*proU*)*600* Δ(*proP-melAB*)*212*) (*14*). Each strain contained plasmid pDC79 (a derivative of pBAD24 (*41*) encoding wild type ProP (*27*)), pDC80 (a derivative of pBAD24 encoding ProP-His_6 (*17*)), pDC117 (a derivative of pBAD24 encoding the fully functional cysteine-less variant of ProP-His_6 with amino acid replacements C112A, C133A, C264V and C367A, denoted ProP* (*36*)), or a derivative of one of those plasmids. Plasmids encoding these variants were created by site-directed mutagenesis as previously described (*36*).

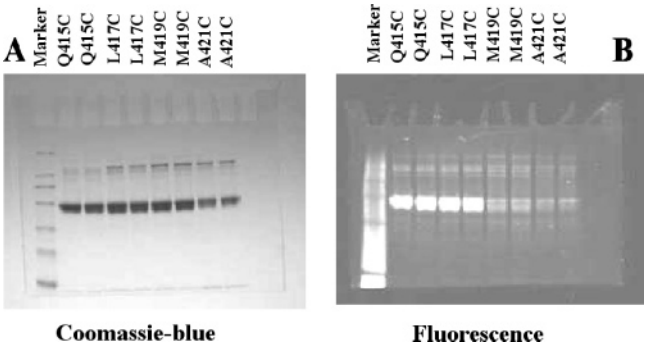

FIGURE 2: Environments of introduced cysteines. Single Cys ProP* variants were cultured with arabinose (*30*) to induce *proP* expression from vector pBAD24. Cell membranes were prepared by osmotic lysis and labeled with anionic, membrane-impermeant dye OGM with freeze−thawing to permeabilize them. The labeled ProP* variants were purified for SDS−PAGE by Ni-NTA affinity chromatography. OGM labeling of the Cys in each variant was assessed as the ratio of the density of the fluorescence (panel B) to the Coomassie Blue-staining (panel A) expressed relative to that ratio for ProP*-Q415C. A representative gel is shown for variants Q415C, L417C, M419C, and A421C, each run in duplicate.

Transport Assays. Published procedures were used to cultivate bacteria in NaCl-free MOPS medium, to measure proline uptake (*18*), and to determine the expression levels of ProP* and its variants in intact bacteria (*27*). Transport assay media were adjusted to the indicated osmolalities with NaCl. For the data reported in Figure 3, a_L and a_H were measured in media supplemented with 50 mM and 170 mM NaCl to attain osmolalities of 0.24 mol/kg and 0.49 mol/kg, respectively. All transport measurements were performed in triplicate on at least two separate days. Figures show means and standard errors of the mean for representative triplicate assays.

Unlike the other variants, ProP*-P420C and ProP*-A428C were expressed at a lower level than ProP* even after the encoding open reading frame was subcloned into pBAD24 to ensure that no mutations had been introduced to the vector inadvertently during site-directed mutagenesis (data not shown). The concentration of arabinose required to restore those variants to levels comparable with ProP* was therefore determined to be 17 μM (procedure previously described (*30*)). Arabinose was added at that concentration to the growth media for the relevant strains.

Site-Directed Fluorescence Labeling. The reactivity of cysteine residues in ProP*-His_6 variants to OGM was determined by site-directed fluorescence labeling of membranes as previously described (*36*). For site-directed fluorescence labeling, expression of ProP* variants was induced by adding L-arabinose to culture media at a final concentration of 13.3 mM. Expression of each variant was indicated from the recovery of purified protein following the labeling procedure. All variants were overexpressed similarly to ProP* except ProP*-A428C, which was expressed at a lower level.

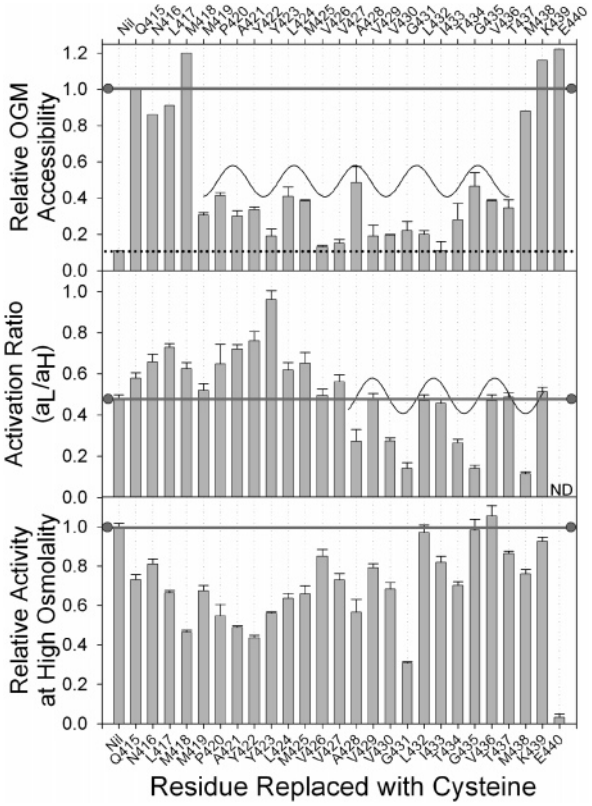

FIGURE 3: Cysteine scan of TM XII. Top panel: The OGM reactivity of Cys introduced to TM XII was investigated as described in the legend to Figure 2. The superimposed sinusoid illustrates the period characteristic of α-helices (3.6 residues per turn). The dotted line indicates the background labeling observed with ProP* (cysteine-less ProP). Middle and bottom panels: Initial rates of proline uptake into bacteria harboring single-Cys ProP* variants were determined at low (a_L) and high (a_H) osmolalities as described in Experimental Procedures. The osmotic activation ratios (a_L/a_H for each variant) are reported in the middle panel with a sinusoid illustrating the period characteristic of α-helices (3.6 residues per turn). No activation ratio could be determined for ProP*-E440C since its activity was negligible (ND is not determined). The relative activities of the variants at high osmolality (a_H for each variant divided by a_H for ProP*) are reported in the bottom panel. Error bars represent standard errors of the means. ProP* and its variants were expressed to similar levels as determined by Western blotting (see Experimental Procedures).

The membranes were suspended in 20 mM K phosphate, pH 8.0 and permeabilized by freeze−thawing in the presence of 40 μM OGM to label Cys accessible from both the cytoplasmic and periplasmic sides. Freeze−thawing had no effect on labeling of a periplasmic Cys residue. ProP variants were purified as described (*41*) and then immediately analyzed by denaturing SDS−PAGE by loading 20 μL aliquots in duplicate lanes onto two 12% gels. The band fluorescence was determined by exposure to UV light, and each gel was also stained for protein using Coomassie Brilliant Blue and imaged using a white light source. Band intensities on the gels were determined by densitometry, the ratio of UV fluorescence to protein for each lane was calculated, and the values of the four lanes from the two gels for the same strain were averaged. Care was taken to ensure that intensities of fluorescent and stained bands were within the linear range by loading different amounts of sample on the gels in preliminary experiments. The standard deviation for the quadruplicate samples was very low and is not shown. The OGM reactivity of each protein was expressed as the relative value of its ratio of densities of fluorescent and Coomassie Blue-stained bands normalized to that of ProP*-Q415C. Most experiments were repeated at least once using a different culture sample. The ratios from two different experiments were averaged to give the mean ± range reported in Figure 3. Cys-less ProP* was also labeled to determine background labeling.

In Vivo Cross-Linking. Cross-linking of ProP variants was carried out *in vivo* in cells expressing the ProP* variants at physiological levels (no arabinose induction), as described (*30*), with minor modifications. An *E. coli* strain expressing ProP* or its variant was initially grown as a 2 mL overnight culture in LB broth (*37*). The preculture (0.25 mL) was used to inoculate 25 mL of LB broth. The subcultures were then incubated a further 3 h at 37 °C with aeration. Aliquots of cells grown in LB medium with no arabinose (10 mL) were transferred to 30 mL Corex tubes prewarmed to 20 °C. DTME was added to give a final concentration of 400 μM. The samples were incubated at 20 °C for 10 min with shaking, followed by addition of 0.5 mM MTSEA, and 10 min further incubation. Cells were then washed once with LB medium.

Following cross-linking, cells were pelleted by centrifugation and resuspended in 1 mL of 100 mM potassium phosphate buffer, pH 7.4. Protein concentrations of these suspensions were determined using a BCA Assay Kit (Pierce, Rockford, IL), using bovine serum albumin (2 mg/mL) as the standard. Cell samples were mixed with sample loading buffer without β-mercaptoethanol, incubated for 15 min at 37 °C, and passed through 30 gauge needles (1/2 CC insulin syringes, BD Consumer Health Care, Oakville, ON, Canada) several times. Protein (5−10 μg) was loaded onto 12% Novex Tris-glycine precast gels (Invitrogen, USA), resolved via SDS−PAGE, and the proteins detected via Western blotting as described (*27*). The amounts of monomer and dimer were quantified by densitometry of Western blots developed using an anti-pentaHis-HRP conjugate (Qiagen Inc., Mississauga, ON, Canada) and an ECL-Plus visualization system.

RESULTS

Refinement of the Homology Model for ProP. Our published model for ProP (PDB 1Y8S (*23*)) was based on an alignment of the ProP sequence and its close paralogues KgtP and ShiA, with GlpT (*24*) and LacY (*26*) as candidate templates. The overall distribution of charged and nonpolar residues was more consistent with that of GlpT, and the model of ProP was therefore based on GlpT as structural template. ProP only has 17% of residues identical to the GlpT sequence, which would not be sufficiently reliable for homology modeling of most globular proteins. For ProP, the validity of the alignment was substantiated by predicting locations of helices and their transmembrane segments with PSIPRED (*42*) and MEMSAT2 (*43*), respectively, and comparing them with actual locations in the structure of GlpT. Additional fine-tuning was done by adjusting the alignment of individual helices to accommodate the observed preference for large hydrocarbon side chains to be in contact with the lipid acyl chains of the bilayer, and to exclude hydrogen-bonding and charged residues from these positions.

We have subsequently re-examined the alignment of ProP onto GlpT by constructing multiple sequence alignments of

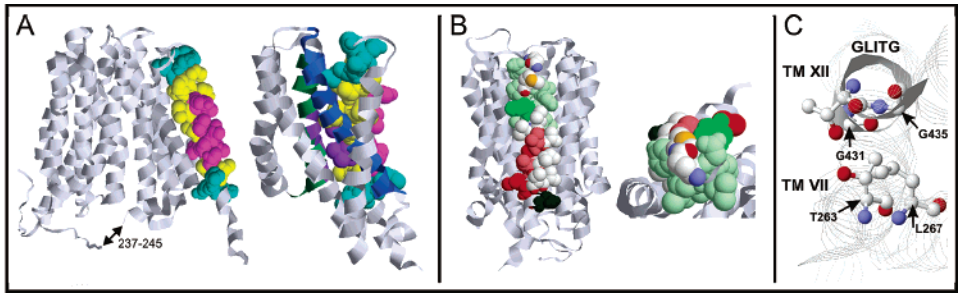

FIGURE 4: Structure−function relationships for ProP. Panel A, solvent exposure of TM XII. Left: OGM labeling of single Cys ProP* variants substantiated the solvent exposure of residues in TM XII predicted by the homology model (*23*). Cys at positions 415−418 or 437−440 (aqua) were fully reactive with OGM and hence solvent exposed whereas Cys at positions 419−436 (pink and yellow) were much less reactive with OGM and hence buried within the membrane. Right: Residues 251−452 are shown with ribbon representations of TMs VIII, X, and XI in gray, TM VII in blue, and TM IX in green and purple (ribbon). The OGM reactivities of Cys residues in TM XII within the membrane, depicted by space filling models, also varied. Those in TM XII colored pink/purple (space filling) and yellow were labeled to extents less than 30% and between 30%-49% of that of ProP*-Q415C, respectively. Hydration of or access to residues 429 and 432 in TM XII is restricted by adjacent residues 328,332,335 and 336 in TM VII (all colored purple). In addition, the periplasmic halves of helices VII, IX, and XII are more widely spaced than their cytoplasmic halves. Panel B, sensitivity of osmotic activation to Cys replacement within TM XII. TM XII is viewed from the membrane (left) and the periplasm (right). TM XII residues are colored to represent the impact of Cys substitution on the activity (a_H) and osmotic activation ratio (a_L/a_H) of the resulting ProP* variant. All ProP* variants except ProP*-E440C showed at least 30% of the activity of ProP* (Figure 3). ProP*-E440C (black) was inactive. Cys substitution of some residues in the periplasmic half of TM XII raised a_L/a_H above 0.6 (green; Y423 dark green) whereas Cys substitution of some residues in the cytoplasmic half of TM XII reduced a_L/a_H below 0.4 (red; G431, G435, and M438 dark red) (see Figure 3). These effects are likely to reflect a decrease and an increase in the osmolality required to activate ProP*, respectively (see Figure 4). Panel C, the putative TM XII−TM VII interface. According to the homology model (*23*) (panel A), the two glycine residues of a GXXXG motif (*35*) in TM XII (G_{431}LITG$_{435}$, gray ribbon) pack against adjacent residues T263 and L267 in TM VII. Cys substitution for G431, T434, or G435 would disrupt this helix packing and/or possibly associated hydrogen bonding. It elevates the osmolality required for ProP activation (Figures 3 and 6).

30 ProP homologues and 5 GlpT homologues. The reliability of multiple sequence alignments improves with increasing number of sequences because the algorithm can detect where variation is tolerated and where conservation is more stringent (*44*). This reanalysis has confirmed our original fine-tuning adjustments, in particular for TM IV and TM XII, and only in TM I was a small modification of alignment suggested.

Solvent Exposure of TM XII Residues. To further test our homology model, we assessed the solvent exposure of TM XII residues by determining the reactivity of introduced cysteines with the negatively charged reagent Oregon Green Maleimide. The environments of residues in the region predicted to encompass TM XII were determined by replacing residues 415−440 singly with Cys, in the background of Cys-less ProP*, and labeling each Cys with OGM in permeabilized membranes. Cys in a hydrophobic environment are not reactive (*45*, *46*), and this approach, using OGM or other Cys-reactive labels, has been used to delineate transmembrane boundaries in other proteins (*45*, *47*, *48*).

OGM labeling of the Cys in each variant was assessed as the ratio of the density of the fluorescence (panel B in Figure 2) to the Coomassie Blue staining (panel A, Figure 2), expressed relative to that ratio for ProP*-Q415C. This representative experiment shows that the Cys residues at positions 415 and 417 were highly reactive with OGM, whereas those at positions 419 and 421 were not. This suggested a change from a polar environment for residue 417 to an apolar environment for residue 419. Proteins with the electrophoretic mobility of dimeric ProP (*30*) were evident in all samples except ProP*-Q415C and ProP*-N416C (e.g., the ProP* variants with Cys at positions 417, 419, and 421 but not 415 in Figure 2). The dimer bands were not included during densitometric analysis of ProP labeling by OGM.

The normalized ratios for all Cys substitutions are shown in Figure 3, top panel. For comparison, the ratio due to background labeling of Cys-less ProP*, probably resulting from the reaction of OGM with Lys residues on the cytoplasmic face (*36*), was 0.11 (dotted horizontal line). The labeling ratio was highest, and close to 1, for residues 415−418 on the periplasmic side and 438−440 on the cytosolic side. It dropped sharply to below 0.4 for residue 419 and residue 437, and was relatively low for all residues in between, indicating that the periplasmic boundary of TM XII was between residues 418 and 419, and the cytoplasmic boundary of TM XII was between residues 437 and 438. This was predicted by the homology model.

However, labeling of a number of residues in the TM domain was significantly higher than background, reaching 0.4−0.5 for residues 420, 424, 425, 428, and 435. This indicates exposure to water within the protein structure and in the model these residues are adjacent to polar and hydrated residues in TM VII in the interior of the protein (T263, T271, T274, Y281). Similar moderate labeling by NEM and MTSES of TM residues of LacY (*49*), and by fluorescein maleimide of TM residues of EmrE (*50*), has been observed. Even higher labeling of Cys residues in transmembrane domains of some proteins occurs if they face a channel or transport pathway (*46*, *51*, *52*).

Fourier transform analysis of the labeling values for residues 419−437 indicated a periodicity of 3.6. A sinusoid of periodicity 3.6 is superimposed on the labeling data in Figure 3 (top panel), and mostly follows the pattern of side chain exposure expected in a helix. In the predicted structure of ProP, most of the residues with a labeling ratio of less than 0.3 are on the side of the transmembrane helix facing the lipid while those with a labeling ratio of 0.3−0.49 are on the side of the helix facing the protein, and/or at the membrane boundaries (Figure 4A, left), where exposure to

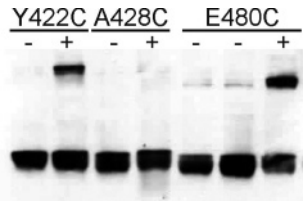

FIGURE 5: Cross-linking of ProP*-Y422C and ProP*-A428C, compared to ProP*-E480C, in intact cells. Cells expressing ProP* variants at a physiological level were incubated in the presence (+) of DTME (0.4 mM) or solvent control (−) as indicated, followed by addition of MTSEA (0.5 mM) in all cases. Whole cell extracts (5−10 μg of protein) were loaded onto 12% gels, resolved by SDS−PAGE, and the proteins detected by Western blotting.

water may occur. An exception is in the region of the unreactive residues 429 and 432, which also face toward the protein. In the model, these residues are in contact with other nonpolar residues in adjacent helices TM IX and TM X, and thus would not be hydrated. They are in a tightly packed region of the structure where TM XII packs against TM IX, with V328, S332, L335, and F336 on the side of TM IX facing TM XII (Figure 4A, right). F368 and M372 are on the side of TM X facing these residues in TM XII.

Cross-Linking of TM XII Residues. We showed earlier that ProP*-E480C, with a Cys in the coiled-coil region of the C-terminal, could be cross-linked by dithio-bis-maleimidoethane (DTME) *in vivo*, indicating that ProP forms a dimer (*30*). DTME is a Cys-reactive, membrane-permeant, homobifunctional, and cleavable reagent. As noted above, dimeric protein was observed in the absence of DTME when ProP* variants containing Cys in TM XII at positions 417−440 and in the C-terminal tail at position 480 were overexpressed and OGM labeled. Much less dimer was seen when Cys was introduced at most other positions and ProP was overexpressed (*23*) and when these TM XII variants were expressed at physiological levels. In order to determine if residues in TM XII are located at the dimer interface, TM XII variants which were labeled by OGM above background levels were treated with DTME *in vivo*.

The results of a typical experiment are shown in Figure 5. A dimer band with an apparent M_r a little greater than that of ProP*-E480C (approximately 90 kDa) was observed for ProP*-Y422C. Where dimer was observed for various Cys substitutions in TM XII, a band of similar mobility was seen. However, no dimer band was seen for ProP*-A428C. DTME cross-linked 20−30% of the ProP protein for ProP* variants containing Cys at positions 419, 420, and 422. These residues are all near the N-terminal, periplasmic end of TM XII (Table 1) and moderately reactive with OGM due to their location near the membrane interface, but predicted to face the lipid. The lack of cross-linking of ProP* containing Cys at position 428 was expected, even though it was reactive with OGM, because it faces toward the interior of the protein in the model. However, variants containing Cys at positions 434−438 were not cross-linked to a significant extent by DTME even though they were moderately reactive with OGM. These residues are near the C-terminal, cytoplasmic end of TM XII. Cys at positions 437 and 438 were expected to face the lipid and be accessible to another monomer of ProP. Of the variants examined with Cys near the C-terminal end, only ProP*-K439C was cross-linked by DTME. We showed earlier that Cys substitutions for several residues in other regions of ProP (A133, G241, and K473) did not result in cross-linked dimer, indicating that the cross-linking observed is not due to random motion of ProP monomers (*30*).

Table 1: DTME Cross-Linking in Vivo of ProP* Variants with Single Cys Substitutions

	% cross-linked ProP[a]			
	replicate 1		replicate 2	
residue	no DTME	with DTME	no DTME	with DTME
M419C	trace	19 ± 3	6 ± 1	16 ± 2
P420C	trace	28 ± 4	trace	26 ± 5
Y422C	trace	32 ± 4	trace	31 ± 2
A428C	trace	trace	0	trace
T434C	0	0		
G435C	trace	trace		
V436C	trace	trace	4 ± 4	13 ± 3
T437C	0	0		
M438C	trace	trace		
K439C	8 ± 1	24 ± 1	8 ± 6	24 ± 3
E480C	trace	50 ± 2	trace	48 ± 3

[a] Values were determined from density analysis of Western blots in experiments such as those shown in Figure 5. Each value represents the mean ± SD of 3−4 values per replicate experiment. Three different strains including one expressing ProP*-E480C, as a positive control, were examined in each experiment. Cross-linking of ProP*-E480C was very reproducible in 6 different experiments (48.5 ± 1.5) and similar to previously reported results for noninduced cells (*30*); representative values are shown. Replicates for other strains are shown, if carried out. Trace = low density band seen on blot but too low to measure density at exposure times where density of monomer band was within the linear range.

*Impacts of Cys Substitutions on the Activity and Osmotic Activation of ProP**. The ProP* variants prepared for this study were characterized to determine the impact of each Cys substitution on the expression, activity, and osmotic activation of ProP. In this system, expression of ProP or ProP* using vector pBAD24 without arabinose induction yields proline uptake activity comparable to that observed after osmotic induction of chromosomal *proP* in the same genetic background (*53*). In addition, the osmotic activation profiles of ProP and ProP* are the same (*36*). ProP, ProP*, and most variants are expressed at comparable levels as determined by Western Blotting (ref *36* and data not shown). Occasionally the levels of poorly expressed variants must be elevated into the normal range via controlled arabinose induction (in this study, induction was required only for variants ProP*-P420C and ProP*-A428C (see Experimental Procedures)).

Most single Cys ProP* variants showed more than 30% of the activity of ProP* (Figure 3, bottom panel) and the proteins were incorporated in the membrane as indicated by the labeling experiments described above. E440 was revealed to be a critical residue since ProP*-E440C had negligible activity. The activity of ProP*-G431C was also low, possibly for reasons discussed further below.

The osmotic activation ratio (a_L/a_H, Figure 3, middle panel) is independent of transporter expression level and can indicate effects of mutations on the osmotic activation threshold. A high ratio may indicate high activity even at low osmolality whereas a low ratio may indicate activation only at high osmolality.

Most Cys substitutions at the periplasmic end of TM XII elevated a_L/a_H, implying that their thresholds for osmotic

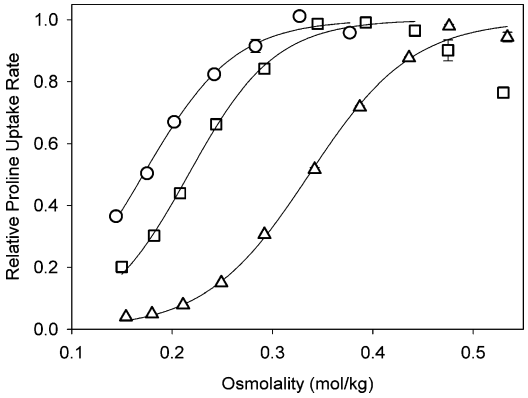

FIGURE 6: Impacts of Cys substitutions on the osmotic activation of ProP*. The initial rate of proline uptake via ProP (squares) and of representative variants with high or low activation ratios (ProP*-Y423C, circles, and ProP*-G435C, triangles, respectively) was measured as described in Experimental Procedures. Rates are expressed relative to the maximum for each variant, and error bars represent standard errors of the mean. Curves are derived by nonlinear regression as described before (*18*). The maximum activities were similar for ProP, ProP*, and ProP*-G435C but lower for ProP*-Y423C (see ref *36* and Figure 3, bottom panel, for relative activities measured at 0.49 mol/kg).

activation were lowered. This interpretation was confirmed for variant ProP*-Y423C (Figure 6). In the homology model, the side chains for residues whose substitution elevates a_L/a_H project in all available directions from the axis of putative TM XII (Figure 4B). Y423, the residue whose Cys substitution had the strongest effect on a_L/a_H, is predicted to face the membrane lipid (Figure 4B). In accord with that prediction, C423 was not reactive with OGM (Figure 3, top panel).

Many of the Cys substitutions at the cytoplasmic end of TM XII reduced a_L/a_H. The interpretation that such substitutions elevate the osmolality required for activation was confirmed for variant ProP*-G435C (Figure 6). The reduction in a_L/a_H showed a 3−4 residue periodicity such that, in the homology model, the residues with the strongest effects on a_L/a_H would cluster on the surface of putative TM XII facing putative TM VII and the membrane (Figure 4B,C). Within this group, a_L/a_H was most profoundly affected by Cys substitution of residues G431 and G435. They delimit a GXXXG motif (*35*) and are expected to form the interface of TM XII with TM VII (Figure 4C). Replacement of a G with a C at this interface may at least locally disrupt packing of helix XII against helix VII. This interaction may normally be stabilized by a hydrogen bond network (the hydroxyl of T263 in TM VII with the hydroxyl of T434 in TM XII and the hydroxyl of T434 in TM XII with the G431 carbonyl). Replacement T434C could further disrupt helix packing by weakening both hydrogen bonds. In contrast M438, the third residue whose substitution strongly depressed a_L/a_H, is part of the next helical turn, more reactive with OGM (Figure 3, top panel) and possibly exposed to the interfacial region on the cytoplasmic surface of the membrane (Figure 4A). It is also near E440, the only residue whose substitution abrogated ProP activity (Figure 3, bottom panel), indicating that this region of TM XII is critical for activity.

DISCUSSION

Our structural predictions are based on a homology model for ProP that is in turn based on the crystal structure of a single, cytoplasm-facing, substrate-free conformation of GlpT (*24*). OGM labeling of ProP was conducted in permeabilized membrane preparations devoid of the proton motive force and the transporter's organic substrates. Thus ProP conformation(s) other than that represented by the structural model may have been present during labeling, and conformations that normally occur during energized substrate transport or substrate exchange may have been absent.

Nevertheless, the labeling data and effects of substitutions on activity strongly support the detailed structure of ProP predicted by the model. These include the membrane boundaries of TM XII, its position on the outside of the protein structure, facing lipid on one side and protein on the other, and the crossing of the cytoplasmic end of TM XII by TM VII on one side and by TMs IX and X on the other side. The labeling data further indicates that water has access to the protein-facing side of the periplasmic end of TM XII. The model suggests that, in the illustrated, cytoplasm-facing conformation, there is more space between the periplasmic halves of TMs XII, VII, IX, and X than the cytoplasmic halves, since all four helices are tilted (Figure 4A, right). Water may also access this region in the outward-facing conformation.

Cys-specific labeling of other proteins such as LacY and a sodium channel (*49*, *54*, *55*) suggests that they may have permanent or transient aqueous crevices and clefts between TM helices that can be accessed by charged and uncharged labels. LacY has a higher rate of H−D exchange than other integral membrane proteins such as bacteriorhodopsin (*56*), suggesting a highly dynamic conformation (*57*, *58*). The periodic labeling of TM XII by negatively charged OGM, despite the predicted location of TM XII on the outside of the protein and not facing the water-filled cavity, suggests a similar dynamic conformation for ProP, with transient opening and closing of helices, allowing water to access the protein-facing residues of TM XII. The moderate labeling of these residues, which is significantly less than the labeling of residues exposed on the periplasmic and cytoplasmic surfaces, indicates that they are not exposed to an aqueous pathway of sufficient size to easily accommodate OGM.

Even though ProP*-E440C was incorporated in the membrane, as indicated by its recovery from the membrane fraction after OGM labeling, this replacement abrogated ProP activity (Figure 3). This result is surprising and warrants further investigation since the model predicts that TM XII is on the lipid-facing ProP surface (Figure 4), the substrate binding site is between the inner surfaces of the two 6-TM bundles, and the H^+ translocation pathway is in the N-terminal 6-TM bundle (*23*). In the model, E440 appears to ion-pair with K439 and/or R444, and is located at the cytoplasmic boundary of the membrane. These ion pairs may be important in positioning TM XII relative to the bilayer. An alternative arrangement of the side chains could couple E440 to R325, which is predicted to be at the cytoplasmic boundary of TM IX. Disruption of any of these ion pairs could affect the overall transport mechanism, and the

presence of Cys at this position could alter the protein's structural dynamics in other ways. The presence of several basic residues in this region may explain why the K439C substitution does not affect activity, in contrast to the E440C substitution.

Cys replacement of the TM VII-facing residues in the cytoplasmic half of TM XII, G431 and G435, elevated the osmolality required for ProP activation. Disruption of the interface between TM XII and TM VII, as discussed above, may prevent or disrupt required conformational changes. However, Cys replacement of residues in the less crowded periplasmic half of TM XII lowered the osmolality required for activation. This occurred for residues facing both the protein and the lipid. Replacement of Y422 and Y423, both of which face the lipid, had the greatest effect on ProP activation. These substitutions may affect hydrogen bonding of the tyrosines with lipid ester groups or the dimerization interface of ProP.

Indeed, variants containing Cys substitutions for Y422, along with M419 and P420, could be cross-linked by DTME, suggesting that they do face the dimer interface. ProP with Cys substituted for Y423 was not examined because it had low reactivity with OGM. These residues are exposed to the lipid at the periplasmic end of TM XII. K439, at the cytoplasmic end of TM XII, was also cross-linked, indicating that TM XII participates in the dimerization interface along its entire length. K439 lies at the predicted helix boundary, so the orientation of its side chain may not follow the helical pattern. ProP* containing Cys substitutions for other residues at the C-terminal end of TM XII may fail to cross-link because these residues are not aligned in register at the dimer interface. TM XII appears to participate in the dimerization interface along its entire length even though the cytoplasmic-facing conformation of ProP is predicted to be pyramidal. One possibility is that the two subunits of the dimer are in opposite phases of the transport cycle and have opposite conformations. Alternatively, monomers in the same conformation could be cross-linked if their transient rocking motions allowed residues that face toward each other in the dimer to be more closely apposed. The length of DTME (13 Å) may also permit cross-linking of residues even if both monomers have the same conformation.

The coiled-coil forming, cytoplasmic C-terminal domain tunes the osmolality range over which ProP activates (*27*, *31*), and it has been implicated in ProP dimerization (*27*−*30*). However, it is absent from at least one ProP orthologue that is an osmosensor and osmoregulator (*31*) and does not appear to function as the osmosensor, per se. Evidence presented here and elsewhere implicates residues within the membrane-integral domain of ProP in osmosensing and the osmoregulation of ProP activity. As for substitutions Y422C and Y423C (Figure 3 and 6), substitutions S62C (periplasmic end of TM II) (*23*) and Y44M (middle of TM I) (J. M. Wood and D. E. Culham, unpublished data) elevate ProP activity at low osmolality, thereby reducing the range over which ProP activity varies. Like substitutions G435C and M438C (Figure 3 and 6), substitution S156C (short cytoplasmic Loop 2) (*23*) dramatically elevates the osmolality required to activate ProP without attenuating the maximum activity attained more than 2-fold. Many other substitutions have little impact on the osmotic activation profile of ProP (Figure 3, (*23*, *36*)). These observations indicate that specific conformational changes to the membrane-integral domain of ProP accompany osmosensing and its osmotic activation. Future efforts will be designed to further delineate those changes.

REFERENCES

1. Roesser, M., and Muller, V. (2001) Osmoadaptation in bacteria and archaea: common principles and differences, *Environ. Microbiol. 3*, 743−754.
2. Roberts, M. F. (2000) Osmoadaptation and osmoregulation in archaea, *Front. Biosci. 5*, D796−D812.
3. Wood, J. M. (1999) Osmosensing by Bacteria: Signals and Membrane-Based Sensors, *Microbiol. Mol. Biol. Rev. 63*, 230−262.
4. Martinac, B. (2001) Mechanosensitive channels in prokaryotes, *Cell Physiol. Biochem. 11*, 61−76.
5. Stein, W. D. (2002) Cell volume homeostasis: ionic and nonionic mechanisms. The sodium pump in the emergence of animal cells, *Int. Rev. Cytol. 215*, 231−258.
6. Hohmann, S. (2002) Osmotic adaptation in yeast−control of the yeast osmolyte system, *Int. Rev. Cytol. 215*, 149−187.
7. Sardini, A., Amey, J. S., Weylandt, K. H., Nobles, M., Valverde, M. A., and Higgins, C. F. (2003) Cell volume regulation and swelling-activated chloride channels, *Biochim. Biophys. Acta 1618*, 153−162.
8. Burg, M. B. (2002) Response of renal inner medullary epithelial cells to osmotic stress, *Comp. Biochem. Physiol., Part A: Mol. Integr. Physiol. 133*, 661−666.
9. Barbier-Brygoo, H., Vinauger, M., Colcombet, J., Ephritikhine, G., Frachisse, J., and Maurel, C. (2000) Anion channels in higher plants: functional characterization, molecular structure and physiological role, *Biochim. Biophys. Acta 1465*, 199−218.
10. Rontein, D., Basset, G., and Hanson, A. D. (2002) Metabolic engineering of osmoprotectant accumulation in plants, *Metab. Eng. 4*, 49−56.
11. Racher, K. I., Voegele, R. T., Marshall, E. V., Culham, D. E., Wood, J. M., Jung, H., Bacon, M., Cairns, M. T., Ferguson, S. M., Liang, W.-J., Henderson, P. J. F., White, G., and Hallett, F. R. (1999) Purification and reconstitution of an osmosensor: transporter ProP of *Escherichia coli* senses and responds to osmotic shifts, *Biochemistry 38*, 1676−1684.
12. Rübenhagen, R., Roensch, H., Jung, H., Krämer, R., and Morbach, S. (2000) Osmosensor and osmoregulator properties of the betaine carrier BetP from *Corynebacterium glutamicum* in proteoliposomes, *J. Biol. Chem. 275*, 735−741.
13. van der Heide, T., and Poolman, B. (2000) Osmoregulated ABC-transport system of *Lactococcus lactis* senses water stress via changes in the physical state of the membrane, *Proc. Natl. Acad. Sci. U.S.A. 97*, 7102−7106.
14. Culham, D. E., Lasby, B., Marangoni, A. G., Milner, J. L., Steer, B. A., van Nues, R. W., and Wood, J. M. (1993) Isolation and sequencing of *Escherichia coli* gene *proP* reveals unusual structural features of the osmoregulatory proline/betaine transporter, ProP, *J. Mol. Biol. 229*, 268−276.
15. Milner, J. L., Grothe, S., and Wood, J. M. (1988) Proline porter II is activated by a hyperosmotic shift in both whole cells and membrane vesicles of *Escherichia coli* K12, *J. Biol. Chem. 263*, 14900−14905.
16. MacMillan, S. V., Alexander, D. A., Culham, D. E., Kunte, H. J., Marshall, E. V., Rochon, D., and Wood, J. M. (1999) The ion coupling and organic substrate specificities of osmoregulatory transporter ProP in *Escherichia coli*, *Biochim. Biophys. Acta 1420*, 30−44.
17. Racher, K. I., Culham, D. E., and Wood, J. M. (2001) Requirements for osmosensing and osmotic activation of transporter ProP from *Escherichia coli*, *Biochemistry 40*, 7324−7333.
18. Culham, D. E., Henderson, J., Crane, R. A., and Wood, J. M. (2003) Osmosensor ProP of *Escherichia coli* responds to the concentration, chemistry and molecular size of osmolytes in the proteoliposome lumen, *Biochemistry 42*, 410−420.
19. Poolman, B., Spitzer, J. J., and Wood, J. M. (2004) Bacterial Osmosensing: roles of membrane structure and electrostatics in lipid-protein and protein-protein interactions, *Biochim. Biophys. Acta 1666*, 88−104.

20. Rübenhagen, R., Morbach, S., and Krämer, R. (2001) The osmoreactive betaine carrier BetP from *Corynebacterium glutamicum* is a sensor for cytoplasmic K^+, *EMBO J. 20*, 5412−5420.
21. Schiller, D., Rübenhagen, R., Krämer, R., and Morbach, S. (2004) The C-terminal domain of the betaine carrier BetP of *Corynebacterium glutamicum* is directly involved in sensing K^+ as an osmotic stimulus, *Biochemistry 43*, 5583−5591.
22. Schiller, D., Krämer, R., and Morbach, S. (2004) Cation specificity of osmosensing by the betaine carrier BetP of *Corynebacterium glutamicum*, *FEBS Lett. 563*, 108−112.
23. Wood, J. M., Culham, D. E., Hillar, A., Vernikovska, Ya. I., Liu, F., Boggs, J. M., and Keates, R. A. B. (2005) Structural model for the osmosensor, transporter, and osmoregulator ProP of *Escherichia coli*, *Biochemistry 44*, 5634−5646.
24. Huang, Y., Lemieux, M. J., Song, J., Auer, M., and Wang, D.-N. (2003) Structure and mechanism of the glycerol-3-phosphate transporter from *Escherichia coli*, *Science 301*, 616−620.
25. Hirai, T., Heymann, J. A., Shi, D., Sarkar, R., Maloney, P. C., and Subramaniam, S. (2002) Three-dimensional structure of a bacterial oxalate transporter, *Nat. Struct. Biol. 9*, 597−600.
26. Abramson, J., Smirnova, I., Kasho, V., Verner, G., Kaback, H. R., and Iwata, S. (2003) Structure and mechanism of the lactose permease of *Escherichia coli*, *Science 301*, 610−615.
27. Culham, D. E., Tripet, B., Racher, K. I., Voegele, R. T., Hodges, R. S., and Wood, J. M. (2000) The role of the carboxyl terminal α-helical coiled-coil domain in osmosensing by transporter ProP of *Escherichia coli*, *J. Mol. Recognit. 13*, 1−14.
28. Zoetewey, D. L., Tripet, B. P., Kutateladze, T. G., Overduin, M. J., Wood, J. M., and Hodges, R. S. (2003) Solution structure of the C-terminal antiparallel coiled-coil domain from *Escherichia coli* osmosensor ProP, *J. Mol. Biol. 334*, 1063−1076.
29. Hillar, A., Tripet, B., Zoetewey, D., Wood, J. M., Hodges, R. S., and Boggs, J. M. (2003) Detection of α-helical coiled-coil dimer formation by spin-labeled synthetic peptides: a model parallel coiled-coil peptide and the antiparallel coiled-coil formed by a replica of the ProP C-terminus, *Biochemistry 42*, 15170−15178.
30. Hillar, A., Culham, D. E., Vernikovska, Ya. I., Wood, J. M., and Boggs, J. M. (2005) Formation of an antiparallel, intermolecular coiled-coil is associated with *in vivo* dimerization of osmosensor and osmoprotectant transporter ProP in *Escherichia coli*, *Biochemistry 44*, 10170−10180.
31. Tsatskis, Y., Khambati, J., Dobson, M., Bogdanov, M., Dowhan, W., and Wood, J. M. (2005) The osmotic activation of transporter ProP is tuned by both its C-terminal coiled-coil and osmotically induced changes in phospholipid composition, *J. Biol. Chem. 280*, 41387−41394.
32. Schiller, D., Ott, V., Kraemer, R., and Morbach, S. (2006) Influence of membrane composition on osmosensing by the betaine carrier BetP from *Corynebacterium glutamicum*, *J. Biol. Chem. 281*, 7737−7746.
33. Peter, H., Burkovski, A., and Krämer, R. (1998) Osmo-sensing by N- and C-terminal extensions of the glycine betaine uptake system BetP of *Corynebacterium glutamicum*, *J. Biol. Chem. 273*, 2567−2574.
34. Biemans-Oldehinkel, E., Mahmood, N. A., and Poolman, B. (2006) A sensor for intracellular ionic strength, *Proc. Natl. Acad. Sci. U.S.A. 103*, 10624−10629.
35. Senes, A., Engel, D. E., and Degrado, W. F. (2004) Folding of helical membrane proteins: the role of polar, GxxxG-like and proline motifs, *Curr. Opin. Struct. Biol. 14*, 465−479.
36. Culham, D. E., Hillar, A., Henderson, J., Ly, A., Vernikovska, Ya. I., Racher, K. I., Boggs, J. M., and Wood, J. M. (2003) Creation of a fully functional, cysteine-less variant of osmosensor and proton-osmoprotectant symporter ProP from *Escherichia coli* and its application to assess the transporter's membrane orientation, *Biochemistry 42*, 11815−11823.
37. Miller, J. H. (1972) *Experiments in Molecular Genetics*, Cold Spring Harbor Laboratory, Cold Spring Harbor, NY.
38. Neidhardt, F. C., Bloch, P. L., and Smith, D. F. (1974) Culture medium for enterobacteria, *J. Bacteriol. 119*, 736−747.
39. Sambrook, J., Frisch, E. F., and Maniatis, T. (1989) *Molecular Cloning: A Laboratory Manual*, 2nd, ed., Cold Spring Harbor Laboratory, Cold Spring Harbor, NY.
40. Kempf, B., and Bremer, E. (1998) Uptake and synthesis of compatible solutes as microbial stress responses to high osmolality environments, *Arch. Microbiol. 170*, 319−330.
41. Guzman, L.-M., Belin, D., Carson, M. J., and Beckwith, J. (1995) Tight regulation, modulation, and high-level expression by vectors containing the arabinose P_{BAD} promoter, *J. Bacteriol. 177*, 4121−4130.
42. Jones, D. (1999) Protein secondary structure prediction based on position-specific scoring matrices, *J. Mol. Biol. 292*, 195−202.
43. Jones, D. T., Taylor, W. R., and Thornton, J. M. (1994) A model recognition approach to the prediction of all-helical membrane protein structure and topology, *Biochemistry 33*, 3038−3049.
44. Thompson, J. D., Higgins, D. G., and Gibson, T. J. (1994) CLUSTAL W: improving the sensitivity of progressive multiple sequence alignment through sequence weighting, position-specific gap penalties and weight matrix choice, *Nucleic Acids Res. 22*, 4673−4680.
45. Ye, L., Jia, Z., Jung, T., and Maloney, P. C. (2001) Topology of OxlT, the oxalate transporter of *O. formigenes*, determined by site-directed fluorescence labeling, *J. Bacteriol. 183*, 2490−2496.
46. Tamura, N., Konishi, S., Iwaki, S., Kimura-Someya, T., Nada, S., and Yamaguchi, A. (2001) Complete cysteine-scanning mutagenesis and site-directed chemical modification of the Tn*10*-encoded metal-tetracycline/H^+ antiporter, *J. Biol. Chem. 276*, 20330−20339.
47. Kimura, T., Shiina, Y., Sawai, T., and Yamaguchi, A. (1998) Cysteine-scanning mutagenesis around transmembrane segment III of Tn*10*-encoded metal-tetracycline/H^+ antiporter, *J. Biol. Chem. 273*, 5243−5247.
48. Xu, Z., O'Rourke, B. A., Skurray, R. A., and Brown, M. H. (2006) Role of transmembrane segment 10 in efflux mediated by the Staphylococcal multidrug transport protein QacA, *J. Biol. Chem.* 792−799.
49. Ermolova, N., Madhvani, R. V., and Kaback, H. R. (2006) Site-directed alkylation of cysteine replacements in the lactose permease of *Escherichia coli:* Helices I, III, VI, and XI, *Biochemistry 45*, 4182−4189.
50. Sharoni, M., Steiner-Mordoch, S., and Schuldiner, S. (2005) Exploring the binding domain of EmrE, the smallest multidrug transporter, *J. Biol. Chem. 280*, 32849−32855.
51. Poelarends, G. J., and Konings, W. N. (2002) The transmembrane domains of the ABC multidrug transporter LmrA form a cytoplasmic exposed, aqueous chamber within the membrane, *J. Biol. Chem. 277*, 42891−42898.
52. Walters, D. E. and Kaplan, R. S. (2004) Homology-modeled structure of the yeast mitochondrial citrate transport protein, *Biophys. J.* 907−911.
53. Wood, J. M. (1988) Proline porters effect the utilization of proline as nutrient or osmoprotectant for bacteria, *J. Membr. Biol. 106*, 183−202.
54. Nguyen, T. P., and Horn, R. (2002) Movement and crevices around a sodium channel S3 segment, *J. Gen. Physiol. 120*, 419−436.
55. Sorgen, P. L., Hu, Y., Guan, L., Kaback, H. R., and Girvin, M. E. (2002) An approach to membrane protein structure without crystals, *Proc. Natl. Acad. Sci. U.S.A. 99*, 14037−14040.
56. Kaback, H. R., Sahin-Toth, M., and Weinglass, A. B. (2001) The kamikaze approach to membrane transport, *Nat. Rev. Mol. Cell Biol. 2*, 610−620.
57. Kwaw, I., Zen, K.-C., Hu, Y., and Kaback, H. R. (2001) Site-directed sulfhydryl labeling of the lactose permease of *Escherichia coli*: Helices IV and V that contain the major determinants for substrate binding, *Biochemistry 40*, 10491−10499.
58. Zhang, W., Hu, Y., and Kaback, H. R. (2003) Site-directed sulfhydryl labeling of helix IX in the lactose permease of *Escherichia coli*, *Biochemistry 42*, 4904−4908.
59. Peter, H., Weil, B., Burkovski, A., Krämer, R., and Morbach, S. (1998) *Corynebacterium glutamicum* is equipped with four secondary carriers for compatible solutes: identification, sequencing, and characterisation of the proline/ectoine uptake system ProP and the ectoine/proline/glycine betaine carrier EctP, *J. Bacteriol. 180*, 6005−6012.

BI062198R